Author(s): Puttreddy, Rakesh; Beyeh, Ngong Kodiah; Ras, Robin H.A.; Trant, John; Rissanen, Kari

Title: Endo-/Exo- and Halogen Bonded Complexes of Conformationally Rigid Cethyl-2-bromoresorcinarene and aromatic N-oxides

Year: 2017

Version:

Please cite the original version:

Puttreddy, R., Beyeh, N. K., Ras, R. H., Trant, J., & Rissanen, K. (2017). Endo-/Exo- and Halogen Bonded Complexes of Conformationally Rigid Cethyl-2-bromoresorcinarene and aromatic N-oxides. CrystEngComm, 19(30), 4312-4320. https://doi.org/10.1039/C7CE00975E

CrystEngComm

Accepted Manuscript

This article can be cited before page numbers have been issued, to do this please use: R. Puttreddy, N. K. Beyeh, R. H.A. Ras, J. Trant and K. Rissanen, *CrystEngComm*, 2017, DOI: 10.1039/C7CE00975E.

ROYAL SOCIETY OF CHEMISTRY

rsc.li/crystengcomm

ROYAL SOCIETY OF CHEMISTRY
View Article Online
DOI: 10.1039/C7CE00975E

Journal Name

ARTICLE

Endo-/*Exo*- and Halogen Bonded Complexes of Conformationally Rigid C-ethyl-2-bromoresorcinarene and aromatic *N*-oxides

Rakesh Puttreddy,[a] Ngong Kodiah Beyeh,[b,c] Robin H. A. Ras,[b] John F. Trant,[c] and Kari Rissanen*[a]

Received 00th January 20xx,
Accepted 00th January 20xx

DOI: 10.1039/x0xx00000x

www.rsc.org/

The host-guest complexes of conformationally rigid C-ethyl-2-bromoresorcinarene with aromatic N-oxides were studied using single crystal X-ray crystallography. Unlike the conformationally more flexible C-ethyl-2-methylresorcinarene, the C-ethyl-2-bromoresorcinarene cavity forms endo-complexes only with the small pyridine-N-oxides, such as pyridine N-oxide, 2-methyl-, 3-methyl- and 4-methylpyrdine N-oxide, and quinoline N-oxide. The larger 2,4,6-trimethylpyridine, 4-phenylpyridine and isoquinoline N-oxide, and 4,4-bipyridine N,N'-dioxide and 1,3-bis(4-pyridyl)propane N,N'-dioxide do not fit into the host cavity. Instead endo-acetone complexes are formed. Remarkably, differing from the anti-gauche exo-complex with C-ethyl-2-methylresorcinarene, the flexible 1,3-bis(4-pyridyl)propane N,N'-dioxide guest forms an anti-anti exo-complex with C-ethyl-2-bromoresorcinarene. The endo- and exo-complexes of C-ethyl-2-bromoresorcinarene and studied N-oxides manifest C-O•••Br, C-H•••π and C-Br•••π interactions.

Introduction

Host-guest supramolecular chemistry is remarkable for the well-defined and predictable nature of the complexes due to designed complementarity.[1] To properly delineate a host molecule's guest preferences, a detailed understanding of the size, shape and conformational behaviour of the host is required. These parameters for any base scaffold can be further modulated by substitution through both the stereoelectronic effects of the substituents and non-covalent interactions driven by the introduced functional groups. Resorcinarenes are macrocyclic host systems that are widely exploited in host-guest chemistry for their bowl-shaped C_{4v} geometry.[2] Synthetic modification at either the upper or lower rim of the resorcinarene bowl induce significant conformational changes, and allow for the required flexibility to access various applications.[2] Finally, the choice of operating solvent and guest molecule can induce further conformational changes in the hosts through either inter- or intramolecular non-covalent interactions; this further increases the complexity of this class of constructs.[2]

Our current campaign is focused on characterizing the host-guest relationships between resorcinarenes and aromatic *N*-oxides.[3] Aromatic *N*-oxides are well-known intermediates for the synthesis of functionalized pyridine compounds.[4] Aromatic *N*-oxides are also very well-established ligands in metal coordination chemistry,[5] and because of this importance, are becoming common guests in host-guest chemistry.[6] However, resorcinarenes as host systems for *N*-oxides remain rare.[3c-f] Recently, we investigated a series of host-guest complexes arising from various aromatic *N*-oxides and *C*-ethyl-2-methylresorcinarenes (MeC2, Fig. 1) by comparing their behavior in both the solution and solid state.[3] From these studies, we found that the C-H•••π interactions lock the host and guest aromatic rings together, with the N-O group positioned above the upper rim of the resorcinarene bowl. During host-guest complexation processes, the position of *endo*-guests, defined by the distance between the closest non-hydrogen atom of the guest to the centroid of the lower rim carbons of the host, is used to estimate and compare the strength of the affinity interaction within various aromatic *N*-oxides@MeC2 complexes.[3] This knowledge allowed us to tune the coordination sphere of copper(II) by using MeC2 as a protecting group. [3b]

These MeC2-*N*-oxide complexation processes are driven by a combination of both the conformational freedom of the MeC2 cavity and the acidity of the *N*-oxide guests' aromatic hydrogens. The well-established flexibility of MeC2 is mainly due to the sterically undemanding methyl group at the lower rim.[1,2a-c] However, the reduction of the acidity of the hydroxyl group hydrogens due to the electron-releasing 2-methyl substitution should not be overlooked. This property increases the resorcinarene skeleton flexibility by weakening the circular intramolecular O•••H•••O hydrogen bonds (HBs), and intermolecular HBs with adjacent hosts, guests and solvent molecules.[7] In the case of C-ethyl-2-bromoresorcinarene (BrC2), the electron-withdrawing bromines make the OH group hydrogens more acidic, induces stronger intramolecular O•••H•••O hydrogen bonds, thereby increasing relative rigidity of the resorcinarene skeleton.[8,9a]

[a] University of Jyvaskyla, Department of Chemistry, P.O. Box 35, FI-40014 University of Jyvaskyla, Finland. E-mail: kari.t.rissanen@jyu.fi
[b] Aalto University, School of Science, Department of Applied Physics, Puumiehenkuja 2, 02150 Espoo, Finland.
[c] University of Windsor, Department of Chemistry and Biochemistry, Windsor, ON, Canada, N9B 3P4.

† Footnotes relating to the title and/or authors should appear here.
Electronic Supplementary Information (ESI) available: [Crystal structures, crystallographic data CCDC 1551401-1551412]. See DOI: 10.1039/x0xx00000x

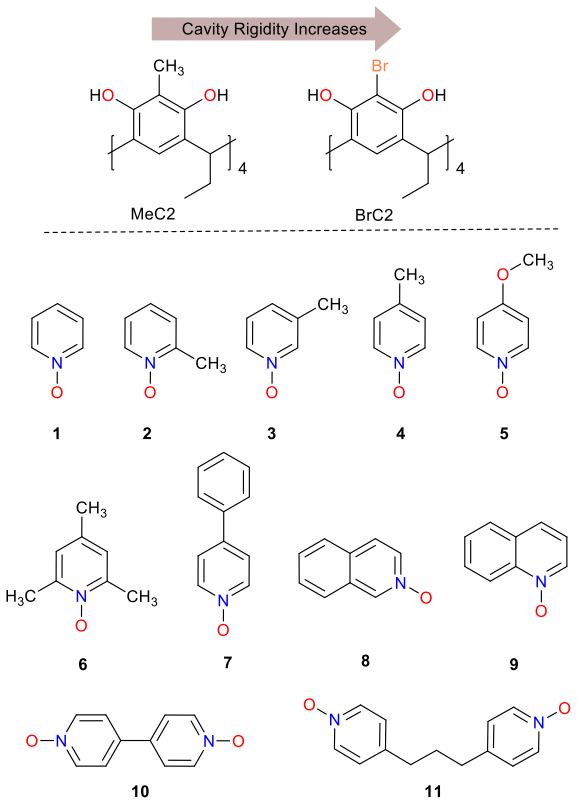

Fig.1 The chemical structures of C-ethyl-2-methylresorcinarene (MeC2) and C-ethyl-2-bromoresorcinarene (BrC2) (on top), pyridine *N*-oxide (**1**), 2-methylpyridine *N*-oxide (**2**), 3-methylpyridine *N*-oxide (**3**), 4-methylpyridine *N*-oxide (**4**), 4-methoxypyridine *N*-oxide (**5**), 2,4,6-trimethylpyridine *N*-oxide (**6**), 4-phenylpyridine *N*-oxide (**7**), isoquinoline *N*-oxide **(8)**, quinoline *N*-oxide (**9**), 4,4'-bipyridine *N,N*'-dioxide (**10**) and 1,3-bis(4-pyridyl)propane *N,N*'-dioxide (**11**).

To improve selectivity of resorcinarene macrocycles for *N*-oxide guests, and to complement our previous studies on flexible electron-rich MeC2 systems, we report here investigation of the interaction of the conformationally more rigid BrC2 with the eleven aromatic *N*-oxides (Fig. 1.). Although resorcinarene host-guest chemistry is a well-established field, the Cambridge Structural Database (CSD) contains only two BrC2 examples (one from our group);[9] consequently, the structural behaviour and host-guest chemistry of this promising electron deficient system remains understudied.[9]

Results and Discussion

The complexes are synthesized by mixing a 1:4 molar ratio of host and guest molecules in acetone at room temperature, heating the reaction mixture to dissolve all the reagents at 50 °C, and then hot-filtering the solution to remove any insoluble aggregates. Slow evaporation of the resulting filtrate provides single crystals suitable for X-ray crystallography. In the case of **11**, attempts to obtain crystals from acetone were unsuccessful; however a 1:1(v/v) mixture of acetone and methanol provided the required crystals. The BrC2 itself crystallized from acetone is a halogen-bonded (XB) complex (Fig. 2), with an asymmetric unit containing two crystallographically distinct acetone molecules. The *endo*-cavity acetone stabilizes 1-D columnar stacks *via endo*- C-H•••π interactions, and C=O•••H interactions with vertically adjacent lower rim hosts. The *exo*-cavity acetone links horizontally adjacent **acetone**@BrC2 units through a μ-*O,O* bidentate halogen bonds with C=O•••Br distances of 2.94 Å [R_{XB} = 0.85].[10]

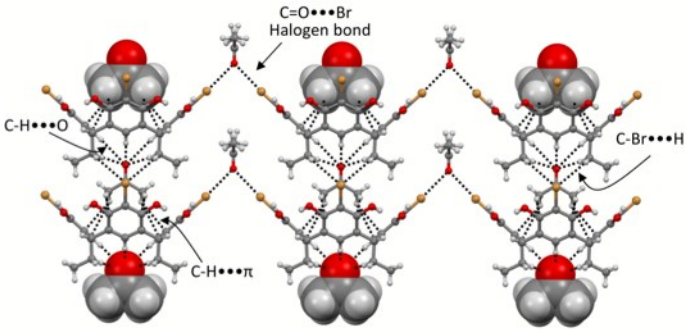

Fig. 2 Section of 1-D polymeric structure of **acetone**@BrC2 to show various non-covalent interactions (black broken lines). Guests are shown both in CPK, and ball & stick models.

Endo- and *exo*-cavity complexes

Complexes with simple pyridine-*N*-oxide (**1**@BrC2), and the *ortho*- and *meta*-methyl substituted derivatives (**2**@BrC2 and **3**@BrC2 respectively) all crystallized in the triclinic space group *P*-1. The asymmetric units contain a host BrC2, and both *endo*- and *exo*-cavity *N*-oxide guests (Fig. 3a-c). Each complex incorporates acetone in the lower rim through C=O•••H-C interactions similar to that in the guest-free **acetone**@BrC2 (Fig. 2). In **1**@BrC2, guest **1** sits inside the cavity at a position of 3.08 Å from the centroid of the lower rim carbon atoms; different from **2**@BrC2 [3.31 Å] and **3**@BrC2 [3.31 Å], suggesting that the increased steric demands of the methyl substituent significantly influence the position of the guest. Interestingly, the two methyl *N*-oxide complexes behave quite similarly as only a slight change in the orientation of the guest is apparently required to compensate for the location of the methyl group. Note that the orientation of *endo*-cavity guests **2** and **3** is *anti*-parallel to the host aromatic rings. The position and effect of the substituent on the aromatic N-oxide guest is clearly observed in **4**@BrC2, where the 4-methyl substituent in **4** resides deeper [2.55 Å] than the para-carbon in guest **1**. Consequently, the C-H•••π interactions[10] in **4**@BrC2 are shorter, and the shortest C-H•••π contacts go from **4**@BrC2 [2.69 Å], through **1**@BrC2 [2.70 Å], and **2**@BrC2 [2.77 Å] to **3**@BrC2 [3.00 Å], as shown in Fig. 3a-d.

The larger guests **5**, **6** and **7** all form *exo*-cavity complexes of the type, (**acetone**@BrC2)•X [where X = **5**, **6** and **7**], where the N-O group interacts directly with the host hydroxyl group [Fig. 3e-g]. The resorcinarene cavities are occupied by acetone molecules stabilized with C-H•••π interactions as seen for **acetone**@BrC2. Clearly, the presence of the three methyl groups in **5** create such a large sterical demand that prevents any possible *endo*-complex. On the other hand, although the geometry of the C-O-CH_3 in **6** is structurally similar to acetone [Fig. S1], and somewhat similar to **4**, the larger –OCH_3 group seems to be incompatible with the small inflexible BrC2 cavity and appears sufficient to prevent *endo*-complexation. In the case of **7** [Fig. 3g], a combination of the rod-like shape of the

ligand and the rigidity of the BrC2 cavity may account for the *exo*-complexation preference.

This cavity intolerance for elongated ligands is also observed for (**acetone**@BrC2)•**8**, (**acetone**@BrC2)•**10** and (**acetone**@BrC2)•**11** [Fig. 3h,j,k]. Guest **9**, quinoline-*N*-oxide, forms an *endo*-complex [Fig. 3i], while isoquinoline-*N*-oxide **8** is structurally too hindered to fit inside the cavity. Moreover, although **9** does reside inside the cavity, the position, 3.75 Å from the centroid of lower rim, suggests that the increased steric bulk of benzo-fused aromatic *N*-oxides interferes with the *endo*-complexation.

Comparison of the host-guest complexes of MeC2 and BrC2. Our recent report showed a good correlation between the single-crystal X-ray structures and calculated Spartan model structures.[3e] We were unable to crystallize BrC2 complexes of 2-picolinic acid *N*-oxide (**12**), *N*-methylmorpholine *N*-oxide (**13**), 2-iodopyridine *N*-oxide (**14**), or 2,2′-bipyridine *N,N*′-dioxide (**15**); however we do not believe that this indicates a failed synthesis. Consequently, using molecular modelling[12] we

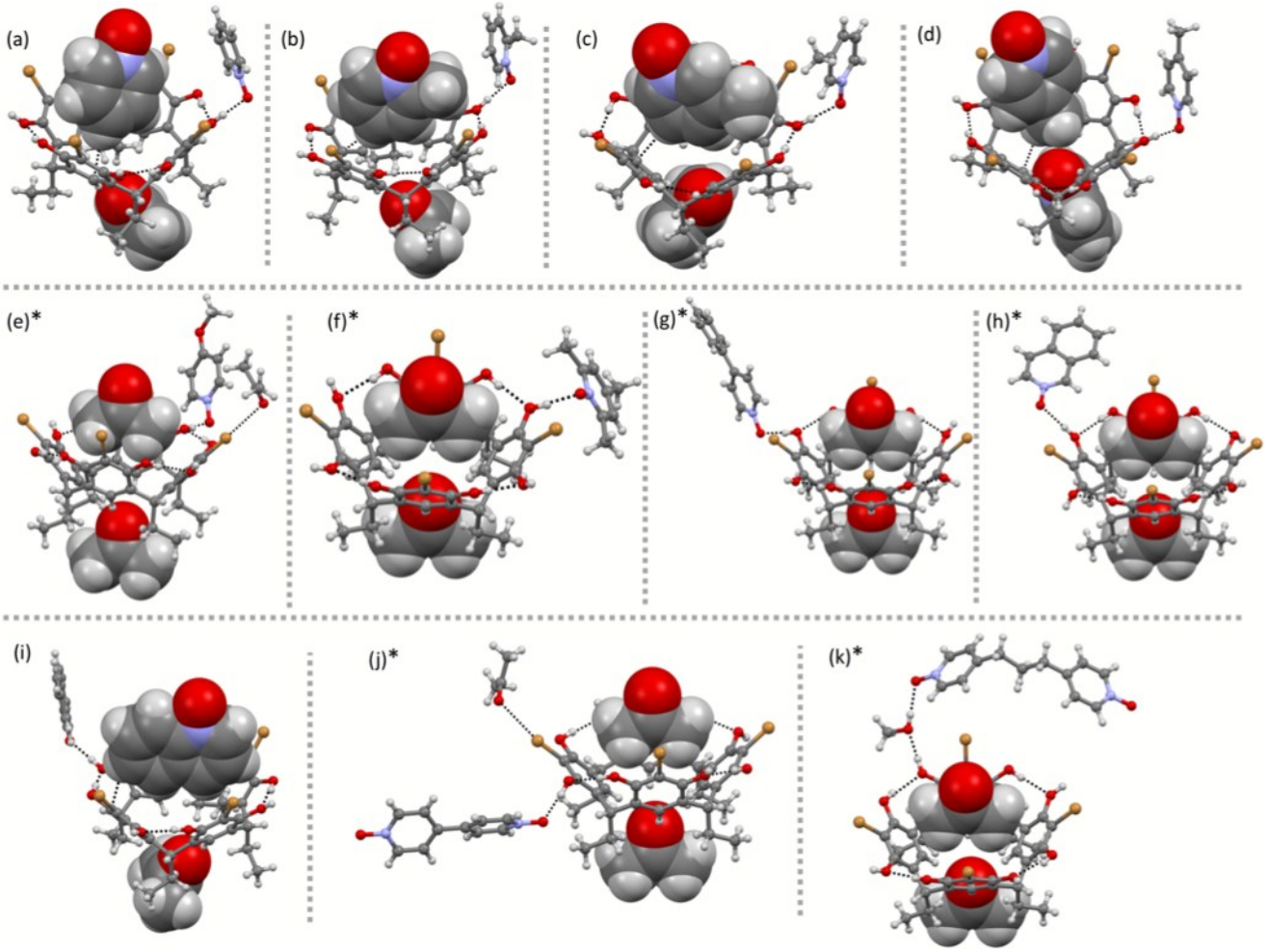

Fig. 3 Top-down views showing the *endo*- and *exo*- complexation in X-ray crystal structures of (a) **1**@BrC2 (b) **2**@BrC2 (c) **3**@BrC2, (d) **4**@BrC2 (e) (**acetone**@BrC2)•5 (f) (**acetone**@BrC2)•**6**, (g) (**acetone**@BrC2)•**7**, (h) (**acetone**@BrC2)•**8**, (i) **9**@BrC2, (j) (**acetone**@BrC2)•**10** and (k) (**acetone**@BrC2)•**11**. The *endo*-cavity and lower rim molecules, either *N*-oxide or acetone, are represented using a CPK model, while the host and *exo*-cavity *N*-oxide guests in ball and stick model. Black broken lines represent O-H•••O and C-H•••π interactions. *The *endo*-cavity and lower rim acetone molecules are crystallographically similar.

calculated the preferred conformation of the complexes of these four ligands with BrC2 along with those formed by the other guest molecules, and compared them with the same parameters obtained when using the more flexible MeC2 system (Table 1). Guests **4**, **6** and **8** were not investigated with MeC2, and their respective host-guest complexation parameters provided in Table 1 were obtained from energy minimized structures rather than crystal structures like the others [Fig. S2]. The difference between the centroid-to-centroid distances of the antipodal aromatic rings [Δ, (B-D)-(A-C)] is used to estimate the relative conformational flexibility during the host-guest complexation of MeC2 and BrC2 [Fig. 4]. These Δ values range between 0.10-2.34 Å for MeC2, and 0.05-1.51 Å for BrC2; the larger Δ values for MeC2 suggest that the cavity is more conformationally flexible for *endo*-complexation than that of BrC2. When the cavity is unable to accommodate the *N*-oxide guest, acetone resides inside BrC2 cavity. These **acetone**@BrC2 units crystallize on centers of inversion, and thus manifesting large Δ values.

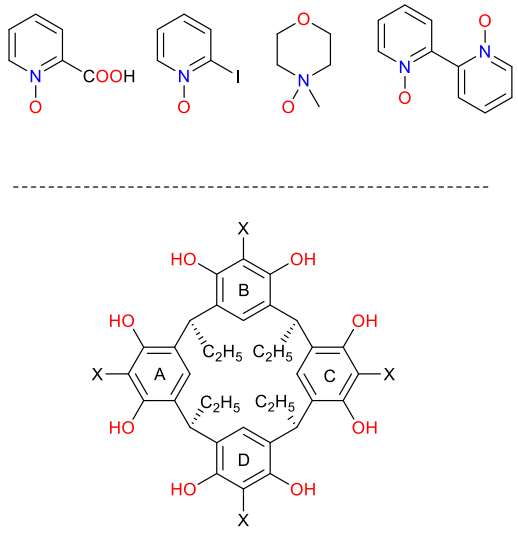

Fig. 4 Representation of C-ethyl-2-substituted resorcinarenes showing the aromatic ring labels used for the molecular modelling discussion; X = CH_3, (MeC2), and X = Br (BrC2)

Table 1 Host-guest *endo*-/*exo*-complexation, and cavity conformation flexibility comparison between MeC2 and BrC2

	When X = CH_3 (Previous study)					
Guest	*endo-* / *exo-*	A-C (*ca.*, Å)	B-D (*ca.*, Å)	Δ [(B-D)-(A-C)]	H (*ca.*, Å)	SC (*ca.*, Å)
1	*endo-*	6.778	6.996	0.218	3.099	2.684[C]
2	*endo-*	6.827	6.923	0.096	2.818	2.678
3	*endo-*	6.226	7.342	1.116	3.127	2.502[C]
4	†*endo-*	6.660	7.135	0.475	3.830	2.974[C]
5	*endo-*	6.815	6.995	0.180	3.055	2.682[C]
6	†*endo-*	6.614	7.191	0.577	3.639	3.053
7	*exo-*	5.826	7.572	1.746	--	--
8	†*endo-*	6.700	7.137	0.437	4.061	2.866
9	*endo-*	6.738	7.090	0.352	2.781	2.673
10	*endo-*	5.560	7.897	2.337	3.938	2.474[C]
11	*endo-*	6.660	7.096	0.436	3.147	2.727
12	*endo-*	6.129	7.429	1.300	2.583	2.578[C]
13	*endo-*	6.624	7.160	0.536	2.924	2.649
14	*endo-*	6.816	6.961	0.145	2.720	2.459[C]
15	*endo-*	6.138	7.734	1.596	2.652	2.442[C]
Guest	When X = Br (Current study)					
1	*endo-*	6.805	6.882	0.077	3.077	2.70[C]
2	*endo-*	6.813	6.860	0.047	3.309	2.766[C]
3	*endo-*	6.751	6.921	0.170	3.312	3.00[C]
4	*endo-*	6.733	6.939	0.206	2.549	2.693[C]
5	*exo-*	6.513	7.133*	0.620	--	--
6	*exo-*	6.433	7.229*	0.796	--	--
7	*exo-*	6.450	7.195*	0.745	--	--
8	*exo-*	6.442	7.245*	0.803	--	--
9	*endo-*	6.746	6.921	0.175	3.749	2.787
10	*exo-*	6.320	7.301*	0.981	--	--
11	*exo-*	6.467	7.221*	0.754	--	--
12	†*endo-*	6.921	6.929	0.008	3.395	2.908
13	†*endo-*	6.771	7.086	0.315	4.076	3.204
14	†*endo-*	6.698	7.114	0.416	3.314	3.0
15	†*endo-*	6.318	7.376	1.058	3.323	2.939[C]

*Centrosymmetric host molecule. †Data obtained from using Spartan software at MM-level.[12] H: Position of the *endo*-cavity guest, calculated from the centroid of the lower rim host carbons to the nearest non-hydrogen atom of the guest. SC: Shortest contact between *endo*-cavity guest and host aromatic ring. SC values with superscript 'C' represent C-H•••π(centroid) shortest contacts while all others are C-H•••C shortest contacts.

The crystal packing

Complexes **1**@BrC2, **2**@BrC2 and **3**@BrC2 form 2-D polymeric sheets, and are all remarkably similar to **1**@BrC2, depicted in Fig.5. The N-O groups of *endo*- and *exo*-guests **1**, **2** and **3** act as bidentate HB acceptors, and bridge adjacent hosts through N-O•••$[(O\text{-}H)_{host}]_2$ interactions [See ESI, Figs. S3-S6]. The complex **4**@BrC2 crystallizes in a 1:3 host-guest ratio, and is the only acetone-free crystal lattice observed in this work. The *endo*- and *exo*-cavity interactions of BrC2 with two molecules of **4** is similar to **X**@BrC2 (X = **1**, **2**, and **3**), however, **4**@BrC2 utilizes an additional third guest **4** in the lower rim as shown in Fig. 3a-d where the others incorporate acetone. The 2-D polymeric sheets of **1**@BrC2 [Fig 5b] and **4**@BrC2 [Fig6b] form dovetail jig pattern when viewed along the *b*- or *c*-axes [Fig 5b,6b], respectively. The 2-D motifs interdigitate to provide the observed 3-D crystal packing, shown as a cartoon in Fig. 6c.

Electronically neutral aromatic *N*-oxides normally show N-O-X (X = metal or hydrogen) interactions in a standard sp^3 tetrahedral geometry; this specific hybridization is well-established in crystal engineering.[13] However, if the aryl ring is sufficiently electron-rich or -deficient, the resulting electronic properties can force the *N*-O group to be better described as an sp^2 N=O or $^{+}N\text{–}O^{-}$, in conjugation with the π-system of the arene, changing the angles of the interaction. This property makes π-systems good candidates for electrostatic interactions, for example, C-Br•••π. In *endo*-complexes **X**@BrC2 (X = **1**, **2**, **3**, **4** and **9**), each host associates with four different *N*-oxide molecules through symmetric (N-O)•••$(O\text{-}H)_{host}$ HB interactions, inducing a shallow cavity around the BrC2 core. The (N-O)•••$(O\text{-}H)_{host}$ hydrogen bonded aromatic rings and bromide of the C-Br bonds favour C-Br•••π interactions,[14] and are highlighted in Fig. 7a-d,g using a double-headed arrow. These are significant interactions, below the sum of the van der Waals radii, with the shortest contacts being *ca.* 3.44 Å (**1**@BrC2), 3.38 Å (**2**@BrC2), 3.36 Å (**3**@BrC2), 3.34 Å (**4**@BrC2) and 3.38 Å (**9**@BrC2). It is interesting to note that these short contacts are established between C-Br and across $(C{=}N^{+}\text{-}O^{-})$ bonds in guests, suggesting that the lone pairs on the bromide and the charge-

View Article Online
DOI: 10.1039/C7CE00975E

separated N^{+}-O^{-} group are responsible for this behaviour. These structures make it clear that the (N-O)•••$(O-H)_{host}$ interactions play vital roles in their solid state 3-D crystal packing.

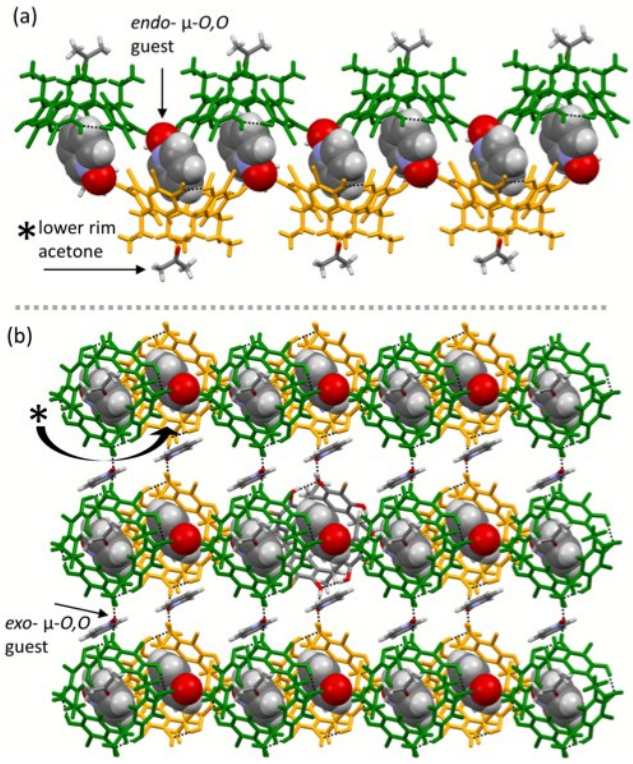

Fig. 5 (a) A 1-D polymeric view of **1**@BrC2 emphasizes the *endo*-cavity and lower rim-associated acetone molecule, (b) 2-D sheet view (90° to the axis in A) to show the *exo*-*N*-oxide and unavailable cavity space (*). Representation: Host in gold, and green capped stick model; *endo*-*N*-oxide in CPK model; *exo*- *N*-oxide and lower rim-associated acetone in capped stick model. Black dashed lines represent HB interactions.

As shown in Fig. 7e, the structure of acetone and the "upper" half of guest **4** are structurally and electronically analogous and interact with hosts' lower rim through similar C=O•••H and N-O•••H interactions, respectively. However, the half of **4** in **4**@BrC2, indicated by '†' [Fig. 6a and 7e], positions inside the lower-adjacent BrC2 cavity assigned as '*' [Fig. 6b] to form C-Br•••π interactions with two aromatic rings as shown in Fig. 7h. The shortest C-Br•••π distances in two π-systems being 3.34 Å and 3.42 Å, respectively. Consequently, the BrC2 cavity and **4** mutually distort from an ideal conformation to accommodate the additional lower rim guest **4**. This hypothesis is supported, and may be explained by: (a) from Table 1, the inter-A-C ring distance attains a maximum spacing of 6.94 Å, a bigger separation than adopted by the other *endo*-complexes; (b) the *endo*-guest **4** positions to the corner as shown in Fig. 7g rather than aligning with the "sides" of the cavity as in Figs. 7a-d; (c) the aromatic rings of *endo*- and lower rim guest **4** deviate from being co-planar with the *exo*-guests [Fig. 7f]; and (d) the adjustment of conformation by **4**@BrC2 initiates C-Br•••Br-C interactions between adjacent hosts at distances of 3.43 Å, an interaction absent in the other complexes due to the smaller amount of inter-host vertical space provided by the lower rim-associated acetone molecule compared to **4** [Fig. 5b, indicated '*'].

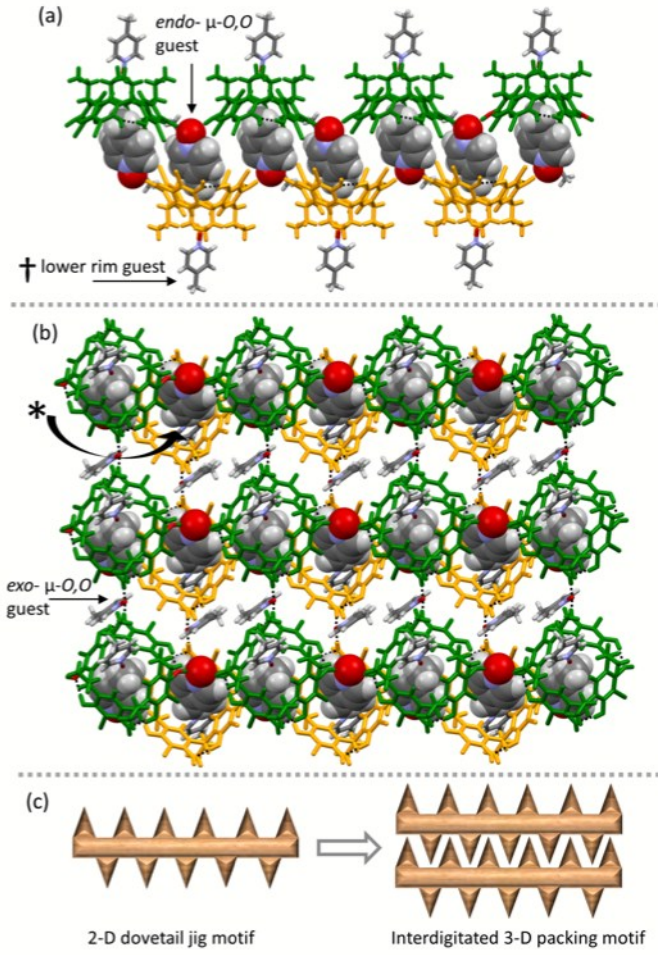

Fig. 6 (a) A 1-D polymeric view of **4**@BrC2 emphasizing the *endo*-cavity and the orientation of the lower rim guest molecules; (b) A 2-D sheet view (axis 90° to that of A) to show the *lower rim N*-oxide (+) and the cavity space (*). Black dashed lines are HB interactions. Representation: Host in gold, and green capped stick model; *exo*-*N*-oxide in CPK model; *exo*- and lower rim *N*-oxide in capped stick model.

Exo-complexes (**acetone**@BrC2)•5 and (**acetone**@BrC2)•6 both contain two crystallographically distinct acetones. In both complexes (Fig. 8a and 8b), one acetone resides inside the cavity, bound by endo- C-H•••π interactions, and stabilizes the 1-D columnar stacks along the *b*-axis through C=O•••H interactions with adjacent lower rim hosts. The crystal is stabilized along the *a*- and *c*-axes by the *exo*-guest **5** and the other acetone molecule. These C-H•••O interactions, driven by aromatic N-oxides, have been heavily exploited for crystal engineering,[13] and they behave as expected in this case. In (**acetone**@BrC2)•**5**, two vertical adjacent hosts extend these columns into 1-D strands, while horizontal host hydroxyl groups orient adjacent units *via* cyclic four-membered O-H•••O interactions to assemble the 2-D structure. These networks are then translated through the *ac* plane by an *exo*-guest **5** and the *exo*-acetone that are connected to host by C-H•••O, and C=O•••Br interactions [Fig. 8a]. The *exo*-acetone is an interesting bidentate HB and XB acceptor displaying $(C-Br)_{host}$•••(O=C)•••(H-

View Article Online DOI: 10.1039/C7CE00975E

C)$_{host}$ interactions at C=O•••Br and C=O•••H distances of 2.32 Å and 3.00 Å (R_{XB} = 0.89), respectively. The 2-D network (Fig. 8a) interdigitate by using intermolecular C-H•••O interactions between neighbouring *N*-oxide guests in the *ac*-plane to generate the 3D crystal lattice. For (**acetone**@BrC2)•**6**, acetone again acts as a bidentate HB and XB acceptor bridge, however, in this case it displays an extended (C-Br)$_{host}$•••(O=C)•••(H-O-H)•••(O-N)$_{guest}$ interactions by incorporating an equivalent of water to form a cyclic ring as shown in Fig. 8b. The C=O•••Br XB contacts were determined to be ca. 3.00 Å long [R_{XB} = 0.89].

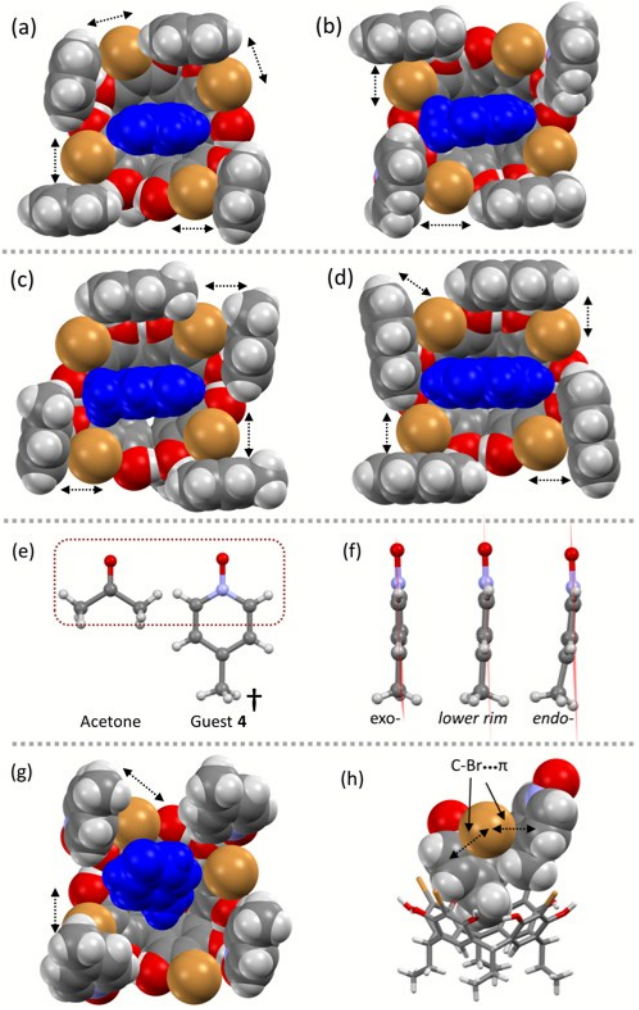

Fig. 7 Complexes (a) **1**@BrC2, (b) **2**@BrC2, (c) **3**@BrC2 (g) **4**@BrC2 and (d) **9**@BrC2 to show C-Br•••π interactions, indicated by double-headed arrows. (f) Aromatic ring planarity comparison of *exo*-, lower rim and *endo*-*N*-oxide in **4**@BrC2. (g) Acetone and guest **4** complexed with BrC2 showing the key C-Br•••O interactions. (h) C-Br•••$(\pi)_2$ Interactions in **4**@BrC2.

The distinct shapes of the guests, and the resulting geometries of the intermolecular HB interactions between host and multidentate acceptor N-O groups, gives rise to a range of different non-covalent interactions for the diaryl systems (**acetone**@BrC2)•X (X = **7**, **8** and **10**). Biphenyl (**acetone**@BrC2)•7 forms a 1-D HB network when viewed along the *b*-axis with adjacent oriented hosts forming O-H•••O four-membered interactions. Perpendicular to this 1-D hydrogen-bonded chain, guest **7** forms a monodentate (O-H)$_{host}$•••(O-N) interaction with an O•••O distance of 2.49 Å. Along the *b*-axis, the 1-D chains are organized *via* the acetones residing in the *endo*-cavity. These molecules facilitate C-H•••π, and C=O•••H interactions with a vertically-adjacent host's lower rim to generate the 1-D columnar stacks. Finally, in the ac-plane, passive guest **7** helps to generate 2-D structures by interdigitating and inducing several C-H•••π and π•••π interactions between BrC2 and guest **7** [Fig. 9b].

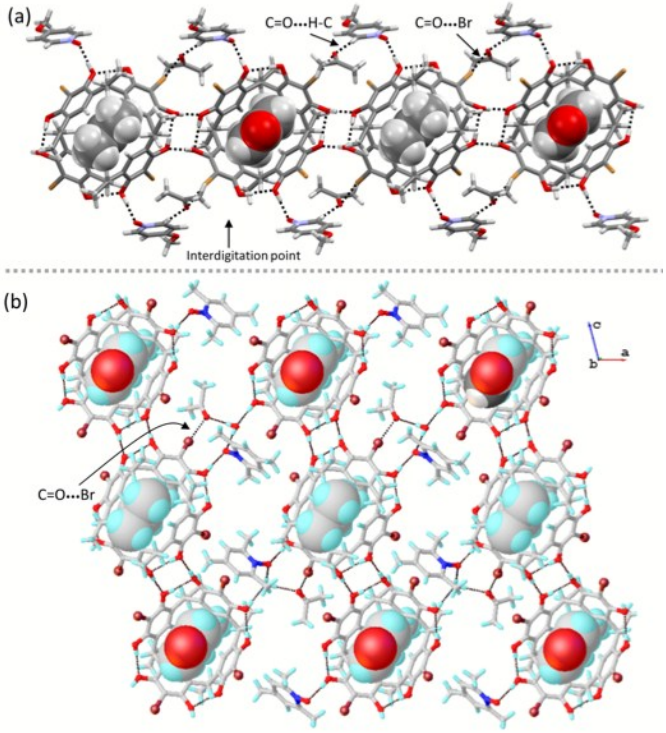

Fig. 8 (a) 1-D Polymer view of (**acetone**@BrC2)•**5** along the *b*-axis. (b) 2-D Sheet view of (**acetone**@BrC2)•**6** along the *b*-axis. Black dashed lines represent HB and XB interactions.

In the isoquinoline-*N*-oxide complex, (**acetone**@BrC2)•8, the N-O group in **8** bridges BrC2 through (O-H)$_{host}$•••(O-N)•••(O-H)$_{host}$ interactions (Fig. 9c), assisting the *endo*-acetone molecules to create the 1-D columnar stacks. The resulting arrangement brings adjacent BrC2 hosts closer together allowing for three distinct C-Br•••π interactions with distances of 3.29 Å, 3.42 Å and 3.48 Å (Fig. 9d). The centrosymmetric *exo*-guest **7** in (acetone@BrC2)•**7** plays the same role as acetone in (acetone@BrC2)•**8**; both reside passively, but close, to the BrC2 host (Fig. 9a&c, red colour capped stick models), and only assist the crystal packing through several long but stabilizing π•••π, C-H•••O and C-H•••π interactions.

Quinoline-*N*-oxide complex **9**@BrC2 crystallizes with two guests per host, similar to the simple **X**@BrC2 (X = **1**, **2**, and **3**) systems. The N-O groups of both the *endo*- and *exo*-cavity **9** molecules are bidentate HB acceptors providing (O-N)•••[(O-H)$_{host}$]$_2$ interactions [Fig. S7]. In (**acetone**@BrC2)•**10**, the external *N,N*'-dioxide **10** bridges adjacent **acetone**@BrC2 units through (O-H)$_{host}$•••(O-N) interactions providing an opportunity for acetone molecules to be accommodated between hosts.

These form stabilizing XBs with C=O•••Br-C distances of 3.23 Å [R_{XB} = 0.96]. As shown in Fig. 9e, the guest N-O group has XB contact with N-O•••Br-C distances of 3.25 Å [R_{XB} = 0.97]. Complex (**acetone**@BrC2)•**10** contains a centrosymmetric passive guest **10**, stabilized through several N-O•••H interactions with nearby acetone and bridging guests **10**.

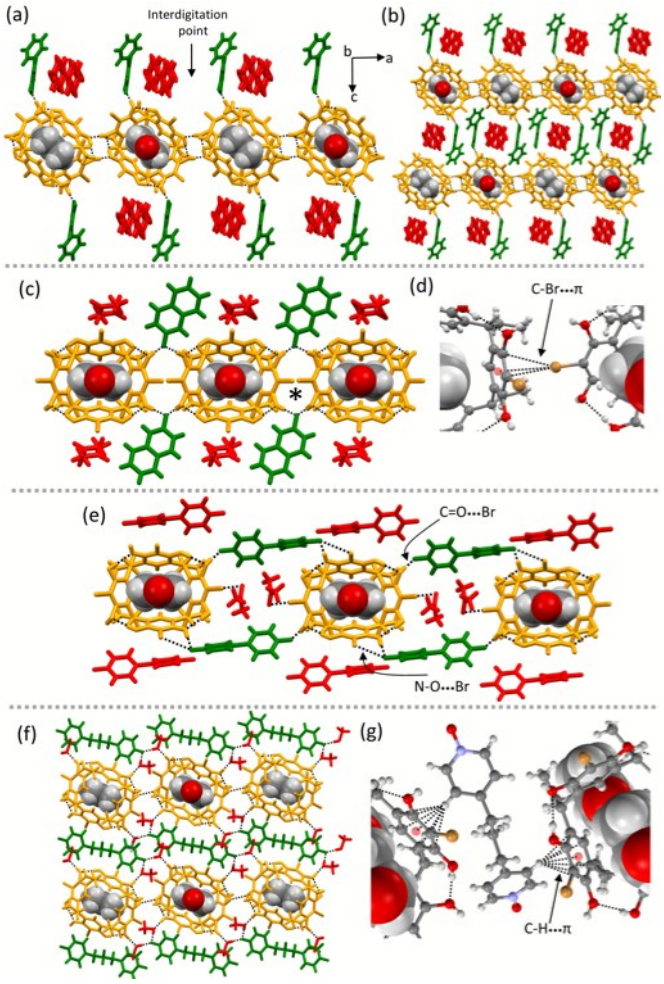

Fig. 9 1-D Polymeric view along the *b*-axis of (a) (**acetone**@BrC2)•**7**; (b) Section of 3-D packing in (**acetone**@BrC2)•**7** to show interdigitation; (c) (**acetone**@BrC2)•**8**; (d) C-Br•••π interactions in (**acetone**@BrC2)•**8**; (e) (**acetone**@BrC2)•**10**; (f) 2-D sheet view along the *b*-axis of (**acetone**@BrC2)•**11**; and (g) an expanded view of the C-H•••π interactions. In all figures, black dashed lines represent HB and XB interactions. Colour representation: Host in gold, hydrogen bonded *N*-oxides in green, and the crystal lattice passive molecules are represented as red capped stick models. The *endo*-cavity acetones are presented as CPK models.

In our recent work focusing on the more flexible MeC2 host,[3e] guest **11** adopted an *anti-gauche* conformation and formed **11**@MeC2 with C-H•••π interactions between the propane chain and the aromatic rings of MeC2. However, in complex (**acetone**@BrC2)•**11**, due to the rigid BrC2 cavity, guest **11** adopts a different *anti-anti* conformation forming an *exo*-complex. This *exo*-centrosymmetric guest is involved in extensive $(N\text{-}O)_{guest}$•••$(H\text{-}OCH_3)$•••$(O\text{-}H)_{host}$ interactions. As shown in Fig. 9f, the aromatic ring of the guest lies close to the BrC2 allowing for short C-H•••π contacts at distances between 2.71 Å and 2.93 Å. More notably, the C-H•••π(centroid) has the shortest contact of 2.50 Å, compared to all the above discussed *endo*- and *exo*- C-H•••π contacts. This further suggests the host aromatic ring is electron deficient.

Conclusions

This study reports and analyzes 13 X-ray crystal structures of the host C-ethyl-2-bromoresorcinarene (BrC2), and its host-guest interactions with aromatic *N*-oxides. The C-ethyl-2-bromoresorcinarene is only capable of forming *endo*-complexes with small aromatic *N*-oxides, *viz.,* pyridine *N*-oxide, 2-methylpyridne *N*-oxide, 3-methylpyridne *N*-oxide, 4-methylpyridne *N*-oxide and quinoline *N*-oxide. Sterically demanding 2,4,6-trimethylpyridine *N*-oxide, 4-phenylpyridine *N*-oxide, isoquinoline *N*-oxide, 4,4-bipyridine *N,N'*-dioxide and 1,3-bis(4-pyridyl)propane *N,N'*-dioxide are unable to be accommodated by the BrC2 cavity, which is occupied by acetone instead. In the guest-misfit complexation process, the acetone molecules organize the hosts to generate 1-D columnar stacks stabilized by *endo*-C-H•••π and lower rim C-H•••O interactions. Including major *endo*- C-H•••π interactions, the weakly polarised C-Br bond displays several C-Br•••π and C-Br•••O halogen bond interactions in the 3-D crystal lattice. The centroid-to-centroid distances between the aromatic rings of C-ethyl-2-bromoresorcinarene and C-ethyl-2-methylresorcinarene (MeC2) were calculated using density functional theory or measured from the X-ray crystal structure to compare the cavities' conformational flexibility. During *endo*-complexation, C-ethyl-2-bromoresorcinarene crystallizes with one complete molecule in the asymmetric unit and maintains a conformationally rigid and small cavity; however, it prefers to act as a centrosymmetric host in *exo*-complexes. As a result, the *exo*-complex host cavities display centroid-to-centroid distances between the aromatic rings greater than those seen in the *endo*-complexes. This small BrC2 cavity forces 1,3-bis(4-pyridyl)propane *N,N'*-dioxide to adopt a more stable *anti-anti* conformation adjacent to the cavity, while it preferred to adopt an *anti-gauche* conformation in its *endo*-complexation with the larger cavity of C-ethyl-2-methylresorcinarene. These two resorcinarenes, BrC2 and MeC2 form a complementary pair as the former is more selective than the latter due to its reduced flexibility and resulting smaller cavity size. This differential selectivity could form the basis for a number of potential diagnostic applications.

Acknowledgements

The authors gratefully acknowledge financial support from the Academy of Finland (RP grant no. 298817, KR: grant nos. 265328, 263256 and 292746; RHAR: grant no. 272579), the University of Jyvaskyla, Aalto University, and the University of Windsor. This work was supported by the Academy of Finland through its Centres of Excellence Programme (HYBER 2014–2019).

References

1 (a) J. W. Steed, and J. L. Atwood, in *Supramolecular Chemistry*, Wiley, Chichester, 2009; (b) J.-M. Lehn, in *Supramolecular Chemistry: Concepts and Perspectives*, Wiley-VCH, Weinheim, 1995; (c) J. L. Atwood and J. W. Steed, *Encyclopedia of Supramolecular Chemistry*, M. Dekker, 2004.

2 (a) P. Timmerman, W. Verboom and D. N. Reinhoudt, *Tetrahedron,* 1996, **52**, 2663–2704; (b) J. Vicens and V. Böhmer, *Calixarenes: A Versatile Class of Macrocyclic Compounds*, Springer Netherlands, 1990. (c) W. Sliwa and C. Kozlowski, *Calixarenes and Resorcinarenes*, Wiley, 2009. (d) V. Böhmer, *Angew. Chem. Int. Ed. Engl.,* 1995, **34**, 713–745; (e) K. Rissanen, *Angew. Chem. Int. Ed.*, 2005, **44**, 3652–3654; (f) J. L. Atwood and A. Szumna, *Chem. Commun.,* 2003, 940–941; (g) J. L. Atwood, L. J. Barbour, and A. Jerga, *Proc. Natl. Acad. Sci.* 2002, **99**, 4837–4841; h) H. Mansikkamäki, C. A. Schalley, M. Nissinen, K. Rissanen, *New J. Chem*. 2005, **29**, 116–127; (i) L. R. MacGillivray, J. L. Atwood, *Chem. Commun.* 1999, **4**, 181–182; (j) N. K. Beyeh, M. Kogej, A. Åhman, K. Rissanen and C. A. Schalley, *Angew. Chem. Int. Ed.* 2006, **45**, 5214–5218.

3 (a) N. K. Beyeh, R. Puttreddy and K. Rissanen, *RSC Adv.*, 2015, **5**, 30222–30226; (b) N. K. Beyeh and R. Puttreddy, *Dalton Trans.*, 2015, **44**, 9881–9886; (c) R. Puttreddy, N. K. Beyeh and K. Rissanen, *CrystEngComm*, 2016; (d) R. Puttreddy, N. K. Beyeh and K. Rissanen, *CrystEngComm*, 2016, **18**, 4971–4976; (e) R. Puttreddy, N. K. Beyeh, R. H. A. Ras and K. Rissanen, *ChemistryOpen*, 2017, DOI: 10.1002/open.201700026; (f) A. Galán, E. C. Escudero-Adán, A. Frontera, P. Ballester, *J. Org. Chem.*, 2014, **79**, 5545–5557.

4 (a) A. Albini, *Heterocyclic N-oxides*, Taylor & Francis, 1991; (b) A. R. Katritzky, J. M. Lagowski, *Chemistry of the Heterocyclic N-Oxides*, Academic Press, 1971.

5 (a) R. Puttreddy and P. J. Steel, *CrystEngComm*, 2014, **16**, 556–560 (*references therein*); (b) R. G. Garvey, J. H. Nelson and R. O. Rasdale, *Coord. Chem. Rev.*, 1968, **3**, 375–407; (b) N. M. Karayannis, L. L. Pytlewski and C. M. Mikulski, *Coord. Chem. Rev.*, 1973, **11**, 93–159; (d) M. Orchin and P. J. Schmidt, *Coord. Chem. Rev.*, 1968, **3**, 345–373.

6 (a) B. Verdejo, G. Gil-Ramírez and P. Ballester, *J. Am. Chem. Soc.*, 2009, **131**, 3178–3179; (b) J. W. Steed, C. P. Johnson, C. L. Barnes, R. K. Juneja, J. L. Atwood, S. Reilly, R. L. Hollis, P. H. Smith and D. L. Clark, *J. Am. Chem. Soc.*, 1995, **117**, 11426–11433; (c) G. Aragay, D. Hernández, B. Verdejo, E. C. Escudero-Adán, M. Martínez and P. Ballester, *Molecules*, 2015, **20**, 16672–16686; (d) A. Shivanyuk and J. Rebek, *Proc. Natl. Acad. Sci.* , 2001, **98**, 7662–7665.

7 (a) H.-J. Schneider, D. Güttes and U. Schneider, *Angew. Chemie Int. Ed. English*, 1986, **25**, 647–649; (b) H. J. Schneider, D. Guettes and U. Schneider, *J. Am. Chem. Soc.*, 1988, **110**, 6449–6454; (c) H. J. Schneider and U. Schneider, *J. Org. Chem.*, 1987, **52**, 1613–1615; (d) H.-J. Schneider and U. Schneider, *J. Incl. Phenom. Mol. Recognit. Chem.*, 1994, **19**, 67–83.

8 R. Puttreddy, N. K. Beyeh, E. Kalenius, R. H. A. Ras and K. Rissanen, *Chem. Commun.*, 2016, **52**, 8115–8118.

9 (a) N. K. Beyeh, D. P. Weimann, L. Kaufmann, C. A. Schalley and K. Rissanen, *Chem. Eur. J.*, 2012, **18**, 5552–5557; (b) J.-M.Bourgeois, H.Stoeckli-Evans, *Helv. Chim. Acta*, 2005, **88**, 2722-2730

10 (a) G. R. Desiraju, P. S. Ho, L. Kloo, A. C. Legon, R. Marquardt, P. Metrangolo, P. Politzer, G. Resnati and K. Rissanen, Pure Appl. Chem., 2013, 85, 1711–1713; (b) O. B. Berryman, A. C. Sather, A. Lledó and J. Rebek, *Angew. Chemie Int. Ed.*, 2011, **50**, 9400–9403; (c) K. Salorinne and M. Nissinen, *CrystEngComm*, 2009, **11**, 1572–1578; (d) D. Cincic and T. Friscic, *CrystEngComm*, 2014, **16**, 10169–10172; (e) V. Nemec and D. Cincic, *CrystEngComm*, 2016, **18**, 7425–7429.

11 C. Janiak, *J. Chem. Soc. Dalt. Trans.*, 2000, 3885–3896.

12 *Spartan'16,* Wavefunction Inc.: Irvine, 2016, USA.

13 (a) G. R. Desiraju, J. J. Vittal and A. Ramanan, *Crystal Engineering: A Textbook*, World Scientific, 2011; (b) E. R. T. Tiekink and J. Zukerman-Schpector, *The Importance of Pi-Interactions in Crystal Engineering: Frontiers in Crystal Engineering*, Wiley, 2012; (c) L. S. Reddy, N. J. Babu and A. Nangia, *Chem. Commun.*, 2006, 1369–1371; (d) M. Muthuraman, R. Masse, J.-F. Nicoud and G. R. Desiraju, *Chem. Mater.*, 2001, **13**, 1473–1479; (e) N. R. Goud, N. J. Babu and A. Nangia, *Cryst. Growth Des.*, 2011, **11**, 1930–1939; (f) G. R. Desiraju, *Acc. Chem. Res.*, 2002, **35**, 565–573; (g) N. J. Babu, L. S. Reddy and A. Nangia, *Mol. Pharm.*, 2007, **4**, 417–434; (h) S. G. Bodige, M. A. Zottola, S. E. McKay and S. C. Blackstock, *Cryst. Eng.*, 1998, **1**, 243–253.

14 (a) M. Albrecht, M. Müller, O. Mergel, K. Rissanen and A. Valkonen, *Chem. – A Eur. J.*, 2010, **16**, 5062–5069; (b) M. Giese, M. Albrecht and K. Rissanen, *Chem. Commun.*, 2016, **52**, 1778–1795; (c) D.-X. Wang and M.-X. Wang, *J. Am. Chem. Soc.*, 2013, **135**, 892–897; (d) M. Giese, M. Albrecht and K. Rissanen, *Chem. Rev.*, 2015, **115**, 8867–8895; (e) K. Fujisawa, M. Humbert-Droz, R. Letrun, E. Vauthey, T. A. Wesolowski, N. Sakai and S. Matile, *J. Am. Chem. Soc.*, 2015, **137**, 11047–11056.

View Article Online
DOI: 10.1039/C7CE00975E

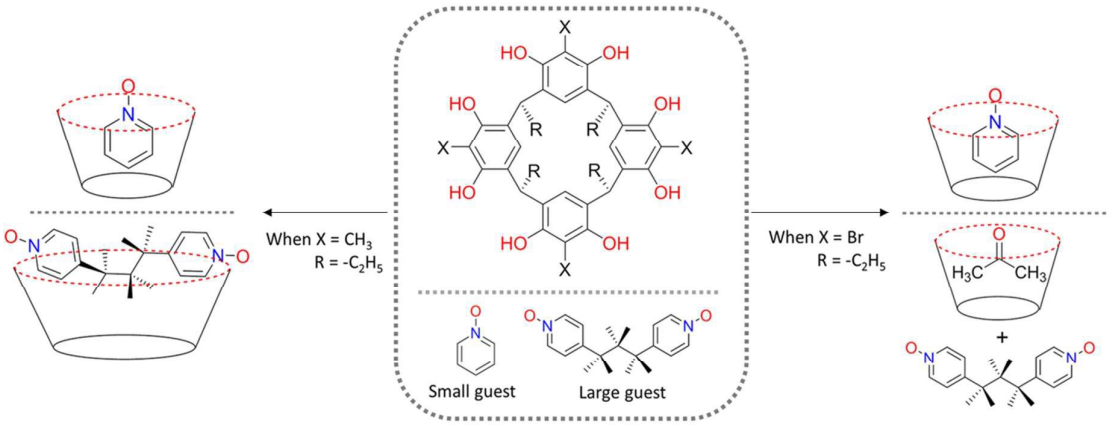

Unlike conformationally flexible C-ethyl-2-methylresorcinarene the structurally more rigid *C4v* cavity in C-ethyl-2-bromoresorcinarene prefers only small aromatic *N*-oxides stabilized through C-H•••π interactions